Proceedings of the 17th World Congress
The International Federation of Automatic Control
Seoul, Korea, July 6-11, 2008

Active Coordination of The Individually Actuated Wheel Braking and Steering To Enhance Vehicle Lateral Stability and Handling ⋆

Erkin Dinçmen * **Tankut Acarman** **

* *Istanbul Technical University, Mechanical Engineering Dept, Inonu Cad., 87 Gumussuyu, TR-34437, Istanbul, Turkey.*
** *Galatasaray University, Computer Engineering Dept, Çırağan Cad., 36, Ortaköy, TR-34357, Istanbul, Turkey.* (tacarman@gsu.edu.tr)

Abstract: In this paper, a novel vehicle dynamics controller is proposed by combining two control loops which are formed by the individually actuated wheel braking and steering regulator. The inner braking loop regulates the individual tire force generation and prevents tire force saturation with respect to tire slip. When the tire forces are regulated to operate in the linear region of their nonlinear characteristics, the drive ability and manageability of the vehicle motion dynamics is enhanced in terms of handling and cornering capability. In the outer loop of the proposed control scheme, Linear Quadratic (LQ) optimal controller is introduced in order to assure the overall lateral stability, the driver's desired yaw rate and the desired trajectory's tracking with the capability of rejecting the disturbance moment acting on the vehicle model in the lateral direction. Simulation results are presented to illustrate the effectiveness of the proposed approach.

1. INTRODUCTION

Electronic Stability Program (ESP) or Vehicle Dynamics Controller (VDC) is becoming standard in today's car technologies. These control systems are introduced to assist to the driver to assure active safety during short-term emergency situations while stabilizing the vehicle motion dynamics, Acarman et al. (2003). VDC helps to the average driver manageability, headway stability and steering ability of the vehicle and it avoids skidding out of the trajectory during short-term emergency maneuvers when the vehicle motion is affected by a maneuver beyond its handling limit, or by side wind force, tire pressure loss, μ-split braking due to different road pavements such as icy, wet and dry pavement. This study may be an extension of the previously developed yaw stability controllers acting on differential braking in combination with the steering compensation with respect to the desired yaw rate calculation, Dincmen and Acarman (2007a), Zanten et al. (1995), Zheng et al. (2006). A side slip angle calculation method has been presented towards more complicated lateral stability controller design replacing the linear controller designed to track the yaw rate reference derived in terms of the longitudinal velocity and the driver steering angle input, Chung et al. (2006) and Fukada (1999). Tire force saturation in the lateral direction or combined tire force generation in both of the lateral and longitudinal direction affects vehicle lateral stability and handling capability. Generation of the tire force in its linear region and preventing its operation in the saturation region, so-called "*unstable region*", is guaranteed by comparing the estimation of the lateral force output with the linearized characteristics in Dincmen and Acarman (2007b). Detecting the possibility of the tire force saturation in the lateral direction, the individually actuated braking actuators are regulated to establish operation in the linear region.

In this paper, a novel VDC is proposed by constituting an hierarchical closed-loop controller acting on the individual wheel braking actuators and steering actuator. In the inner loop, the error variable is defined in terms of the observed deviation of the individual lateral tire force from its linear operating region and tire dynamics are stabilized with lower slip angle values leading to higher tire force generation individually. In the outer loop, to track the driver's desired yaw motion while minimally exciting roll dynamics, an active steering controller algorithm is implemented based on a Linear Quadratic (LQ) optimal formulation. This outer loop assists to the driver for manageability, and steering ability by regulating the vehicle motion in the lateral direction by compensating the possible moment difference which may be caused by different force generation of the individually regulated tires due to different road pavements.

The paper is organized as follows. Control algorithm composed by individual wheel braking and steering regulation is proposed in Section 2. Simulation scenario is presented in Section 3. Section 4 gives some concluding remarks. Stability analysis on a basis of Lyapunov analysis is given in Appendix.

⋆ The second author gratefully acknowledges support of Galatasaray University through research funding. The authors gratefully acknowledge support of the Turkish National Research Council TUBITAK under grant no: 106E121 and support of the European Union Framework Programme 6 through the AUTOCOM SSA project (INCO Project No: 16426).

2. CONTROL ALGORITHM

2.1 Vehicle Model

The equations of motion dynamics for a nonlinear double track vehicle model are given

$$\dot{u} = \frac{Fx_{sum}}{m} + vr - \frac{1}{2}A_\rho |u|u \tag{1}$$

$$\dot{v} = \frac{Fy_{sum}}{m} - ur \tag{2}$$

$$\dot{r} = \frac{Mz_{sum}}{I_z} \tag{3}$$

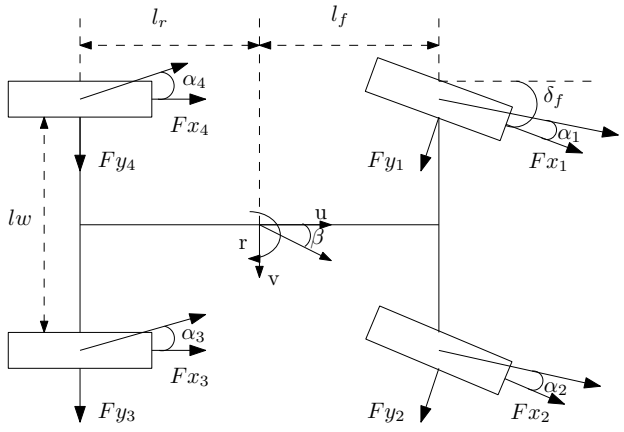

Fig. 1. Vehicle model

where m denotes the vehicle mass, A_ρ is the aerodynamic drag force coefficient, I_z is the yaw inertia, r is the yaw rate, u and v denotes the velocity in longitudinal and lateral direction, respectively, as illustrated in Fig.1. Fx_{sum}, Fy_{sum} and Mz_{sum} are the sum of forces and moment acting on the vehicle model

$$\begin{aligned}
Fx_{sum} &= (Fx_1 + Fx_2)\cos\delta_f - (Fy_1 + Fy_2)\sin\delta_f \\
&\quad + Fx_3 + Fx_4 \\
Fy_{sum} &= (Fx_1 + Fx_2)\sin\delta_f + (Fy_1 + Fy_2)\cos\delta_f \\
&\quad + Fy_3 + Fy_4 \\
Mz_{sum} &= ((Fx_1 - Fx_2)\cos\delta_f - (Fy_1 - Fy_2)\sin\delta_f)\frac{lw_f}{2} \\
&\quad + ((Fx_1 + Fx_2)\sin\delta_f + (Fy_1 + Fy_2)\cos\delta_f)l_f \\
&\quad + (Fx_4 - Fx_3)\frac{lw_r}{2} - (Fy_3 + Fy_4)l_r
\end{aligned}$$

Here δ_f is front wheel steering angle, l_f and l_r is the distance from center of gravity to the front and rear axle, lw_f and lw_r is the front and rear track width, respectively. Tire slip angles are calculated as follows

$$\begin{aligned}
\alpha_1 &= \delta_f - \tan^{-1}\left(\frac{v + rl_f}{u + rlw_f/2}\right) \\
\alpha_2 &= \delta_f - \tan^{-1}\left(\frac{v + rl_f}{u - rlw_f/2}\right) \\
\alpha_3 &= -\tan^{-1}\left(\frac{v - rl_r}{u - rlw_r/2}\right) \\
\alpha_4 &= -\tan^{-1}\left(\frac{v - rl_r}{u + rlw_r/2}\right)
\end{aligned} \tag{4}$$

2.2 Tire Forces

Modelling tire forces along the longitudinal and lateral axes, Dugoff's tire model is used. Dugoff's model may be analytically derived at controller's development stage. Combined longitudinal and lateral force generation are directly related to the tire road coefficient in compact form, for $i = 1, 2, 3, 4$,

$$Fx_i = Cx_i\frac{\kappa_i}{1+\kappa_i}f(\lambda_i) \tag{5}$$

$$Fy_i = Cy_i\frac{\tan(\alpha_i)}{1+\kappa_i}f_i(\lambda_i) \tag{6}$$

where Cx_i and Cy_i are the i-th tire longitudinal and lateral cornering stiffness, respectively. The variable λ_i and the function $f_i(\lambda_i)$ are given,

$$\lambda_i = \frac{\mu Fz_i(1+\kappa_i)}{2\sqrt{(Cx_i\kappa_i)^2 + (Cy_i\tan(\alpha_i))^2}} \tag{7}$$

$$f_i(\lambda_i) = \begin{cases} (2-\lambda_i)\lambda_i & \text{if } \lambda_i < 1 \\ 1 & \text{if } \lambda_i \geq 1 \end{cases} \tag{8}$$

where μ denotes the road friction coefficient. For simplicity, the dynamic weight transfer is neglected and the vertical tire forces are

$$Fz_1 = Fz_2 = \frac{mg}{2}\frac{l_r}{l_f + l_r} \tag{9}$$

$$Fz_3 = Fz_4 = \frac{mg}{2}\frac{l_f}{l_f + l_r} \tag{10}$$

Tire slip ratios are

$$\kappa_i = -\frac{u_{ti} - \omega_i R}{u_{ti}} \tag{11}$$

where ω_i denotes the i-th tire angular velocity, R is the tire effective radius, u_{ti} is the i-th tire velocity on rolling direction, which is is given

$$\begin{aligned}
u_{t1} &= (u + r(lw_f/2))\cos\delta_f + (v + rl_f)\sin\delta_f \\
u_{t2} &= (u - r(lw_f/2))\cos\delta_f + (v + rl_f)\sin\delta_f \\
u_{t3} &= (u - r(lw_r/2)) \\
u_{t4} &= (u + r(lw_r/2))
\end{aligned} \tag{12}$$

2.3 The inner-loop: Individually Actuated Wheel Braking Controller to Avoid Tire Force Saturation

The proposed controller is built on the observation of the deviation between the individual nonlinear tire force and the linear one. The main purpose of this approach is to enforce the tire forces stay in the linear region and to generate high tire force with respect to tire slip improving cornering and handling capability of the vehicle motion dynamics. Even though the tire forces are entered into the saturation region, so-called "*unstable region*", where tire forces outputs decrease while diverging with respect to increasing tire slip angles, the proposed controller intervenes to this undesired transient operation by applying the required individual wheel braking that may recover the tire forces near to the linear region. The nonlinear tire force characteristics for different road friction coefficients

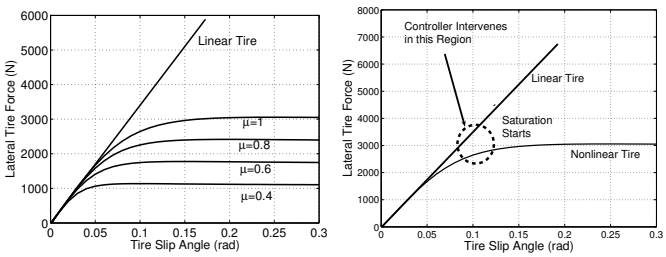

Fig. 2. Left: The lateral tire force characteristics. Right: Braking algorithm to prevent tire force saturation

and the proposed methodology are illustrated in Fig.2. The estimation of front axle and rear axle lateral tire force is based on longitudinal tire forces estimation, lateral acceleration and yaw rate measurement with differential operation (Fukada (1999)). Estimation of tire longitudinal force is based on tire angular velocity measurement, Drakunov, Ozguner et al. (1995). The simplified longitudinal tire dynamics can be written as follows

$$I_w\dot{\omega}_i = T_d - Tb_i - Fx_iR \tag{13}$$

where T_d is drive moment, Tb_i is individual wheel braking moment, I_w is the wheel inertia for $i = 1, 2, 3, 4$. Defining the observer dynamics

$$I_w\dot{\hat{\omega}}_i = T_d - Tb_i + RV_i \tag{14}$$

where $\hat{\omega}_i$ is the estimated individual tire angular velocity, $\bar{\omega}_i = \omega_i - \hat{\omega}_i$ is the tracking error variable and $M > 0$ is a sufficiently large constant, V_i is selected as a discontinuous function

$$V_i = -Msign(\bar{w}_i) \tag{15}$$

Subtracting (14) from (13), one can get

$$I_w\dot{\bar{\omega}}_i = -Msign(\bar{w}_i)R - Fx_iR \tag{16}$$

By choosing $|M| > \max|Fx_i|$, the sliding mode may be enforced, the tracking error is zero and the equivalent value of V_i will be equal to the estimated value. The longitudinal tire force can be estimated from (16)

$$\hat{F}x_i = -Msign(\bar{\omega}_i) \tag{17}$$

To attenuate high frequency, high gain chattering effects caused by infinite frequency switching function, *i.e.* $sign(\cdot)$, a lowpass filter is used to obtain smooth estimated values of individual brake force,

$$\hat{F}x_i(s) = \frac{1}{\tau s + 1}V_i(s) \tag{18}$$

where τ is the time constant of the equivalent value filter to attenuate high frequency effects, Drakunov, Ozguner et al. (1995).

Lateral tire forces may be estimated by summing the forces and moment acting on a single track vehicle model as illustrated in Fig.3,

$$\begin{aligned}\hat{F}y_f = &\Big(l_rma_y + Iz\dot{r} - (\hat{F}x_1 + \hat{F}x_2)\sin\delta_f(l_f + l_r)\\ &+\hat{F}x_2\cos\delta_f lw/2 + \hat{F}x_3lw/2 - \hat{F}x_1\cos\delta_f lw/2\\ &-\hat{F}x_4lw/2\Big)/\Big(\cos\delta_f(l_f + l_r)\Big)\end{aligned} \tag{19}$$

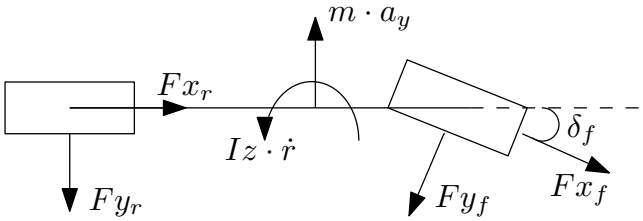

Fig. 3. Forces and moments acting on a single track vehicle model

$$\begin{aligned}\hat{F}y_r = &\Big(l_fma_y - Iz\dot{r} + \hat{F}x_4lw/2 - \hat{F}x_3lw/2\\ &-\hat{F}x_2\cos\delta_f lw/2 + \hat{F}x_1\cos\delta_f lw/2\Big)/\Big(l_f + l_r\Big)\end{aligned} \tag{20}$$

where $\hat{F}y_f$ and $\hat{F}y_r$ denotes the estimated variable of front and rear axle total lateral force and a_y is the lateral acceleration. $\hat{F}x_f$ is the estimated front axle total longitudinal force, which is calculated as follows

$$\hat{F}x_f = \hat{F}x_1 + \hat{F}x_2 \tag{21}$$

The error between the nonlinear front axle lateral force and its linearized value is defined

$$e_f = Fy_{flin} - Fy_f \tag{22}$$

$$e_f = Cy_f\alpha_f - Cy_1\frac{\tan\alpha_1}{1+\kappa_1}f_1(\lambda_1) - Cy_2\frac{\tan\alpha_2}{1+\kappa_2}f_2(\lambda_2) \tag{23}$$

here Fy_f is front axle total lateral force, Fy_{flin} its linearized value, Cy_f front axle total cornering stiffness and α_f front axle slip angle which is calculated as in (24).

$$\alpha_f = \delta_f - \beta - \frac{l_fr}{u} \tag{24}$$

Along the controller development, the vehicle longitudinal velocity u and vehicle side slip angle β is assumed to be estimated (Fukada (1999)) whereas the yaw rate and steering angle is assumed to be measured. The time-derivative of the error given by (22) may be derived

$$\begin{aligned}\dot{e}_f = &Cy_f\dot{\alpha}_f - Cy_1\frac{\dot{\alpha}_1(1+\kappa_1)}{\cos^2\alpha_1(1+\kappa_1)^2}f_1(\lambda_1)\\ &- Cy_2\frac{\dot{\alpha}_2(1+\kappa_2)}{\cos^2\alpha_2(1+\kappa_2)^2}f_2(\lambda_2)\\ &+ Cy_1\frac{\tan\alpha_1}{(1+\kappa_1)^2}f_1(\lambda_1)\dot{\kappa}_1 + Cy_2\frac{\tan\alpha_2}{(1+\kappa_2)^2}f_2(\lambda_2)\dot{\kappa}_2\\ &- Cy_1\frac{\tan\alpha_1}{1+\kappa_1}\frac{\partial f_1}{\partial\lambda_1}\dot{\lambda}_1 - Cy_2\frac{\tan\alpha_2}{1+\kappa_2}\frac{\partial f_2}{\partial\lambda_2}\dot{\lambda}_2\end{aligned} \tag{25}$$

Deriving $\dot{\kappa}_i$ in terms of the wheel states,for i=1,2,3,4, and reconsidering the tire dynamics given in (13),

$$\dot{\kappa}_i = -(\kappa_i + 1)\frac{\dot{u}_{ti}}{u_{ti}} - \frac{R^2}{I_w}\frac{\hat{F}_{xi}}{u_{ti}} - \frac{R}{I_w}\frac{1}{u_{ti}}T_{bi} \tag{26}$$

Equation (25) can be rewritten as follows

$$\begin{aligned}\dot{e}_f = &Cy_f\dot{\alpha}_f - Cy_1\frac{\dot{\alpha}_1}{\cos^2\alpha_1(1+\kappa_1)}f_1(\lambda_1)\\ &- Cy_1\frac{\tan\alpha_1}{1+\kappa_1}\frac{\partial f_1}{\partial\lambda_1}\dot{\lambda}_1 + \left(Cy_1\frac{\tan\alpha_1}{(1+\kappa_1)^2}f_1(\lambda_1)\right)\end{aligned} \tag{27}$$

$$\cdot \left((\kappa_1 + 1) \frac{\dot{u}_{t1}}{u_{t1}} + \frac{R^2}{I_w} \frac{\hat{F}_{x1}}{u_{t1}} + \frac{R}{I_w} \frac{1}{u_{t1}} T_{b1} \right)$$
$$- Cy_2 \frac{\dot{\alpha}_2}{\cos^2 \alpha_2 (1 + \kappa_2)} f_2(\lambda_2)$$
$$- Cy_2 \frac{\tan \alpha_2}{1 + \kappa_2} \frac{\partial f_2}{\partial \lambda_2} \dot{\lambda}_2 - \left(Cy_2 \frac{\tan \alpha_2}{(1 + \kappa_2)^2} f_2(\lambda_2) \right)$$
$$\cdot \left((\kappa_2 + 1) \frac{\dot{u}_{t2}}{u_{t2}} + \frac{R^2}{I_w} \frac{\hat{F}_{x2}}{u_{t2}} + \frac{R}{I_w} \frac{1}{u_{t2}} T_{b2} \right)$$

Towards controller design, the time-derivative of tire velocities on the rolling direction are simplified as follows:

$$\begin{aligned} \dot{u}_{t1} &= \dot{u} + \dot{r}(lw_f/2) \\ \dot{u}_{t2} &= \dot{u} - \dot{r}(lw_f/2) \\ \dot{u}_{t3} &= \dot{u} - \dot{r}(lw_r/2) \\ \dot{u}_{t4} &= \dot{u} + \dot{r}(lw_r/2) \end{aligned} \tag{28}$$

The longitudinal velocity given by (1) is simplified by neglecting aerodynamic drag force and by small angle assumption:

$$\dot{u} = \frac{\hat{F}x_{total} - \hat{F}y_f \delta_f}{m} + vr \tag{29}$$

where

$$\hat{F}x_{total} = \hat{F}x_1 + \hat{F}x_2 + \hat{F}x_3 + \hat{F}x_4 \tag{30}$$

for i=1,2

$$Tb_i = \left(\frac{I_w}{R} u_{ti} \left(k_{i1} |\dot{\alpha}_f| + k_{i2} |\dot{\alpha}_i| + M_i \right) sign(\alpha_i) - R\hat{F}_{xi} \right.$$
$$\left. - \frac{I_w}{R} (1 + \kappa_i) \left(\frac{\hat{F}x_{total} - \hat{F}y_f \delta_f}{m} + vr + \dot{r} \frac{l_{wf}}{2} \right) \right) \Gamma(e_f)$$

Without loosing of generality, the controller derived to regulate lateral deviation subjected to the front axle may be repeated for the rear axle, defining,

$$\dot{e}_r = \dot{F}y_{rlin} - \dot{F}y_r \tag{31}$$

where Fy_{rlin} is rear axle linearized total lateral force,

$$Fy_{rlin} = Cy_r \alpha_r \tag{32}$$

where Cy_r is rear axle total cornering stiffness, α_r rear axle slip angle calculated as

$$\alpha_r = -\beta + \frac{l_r r}{u} \tag{33}$$

To stabilize the lateral deviation subjected to the rear axle, the controller's outputs are derived, for i=3,4

$$Tb_i = \left(\frac{I_w}{R} u_{ti} \left(k_{i1} |\dot{\alpha}_r| + k_{i2} |\dot{\alpha}_i| + M_i \right) sign(\alpha_i) - R\hat{F}_{xi} \right.$$
$$\left. - \frac{I_w}{R} (1 + \kappa_i) \left(\frac{\hat{F}x_{total} - \hat{F}y_f \delta_f}{m} + vr + \dot{r} \frac{l_{wr}}{2} \right) \right) \Gamma(e_r)$$

The gains k_{i1}, k_{i2} and M_i are chosen to be positive constants to satisfy $e_f, e_r \to 0$ and $\dot{e}_f, \dot{e}_r \to 0$ as $t \to \infty$. Also the discontinuous function $\Gamma(\cdot)$ is a function with deadzone

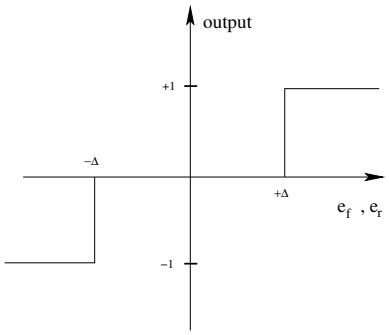

Fig. 4. Function Γ

which is seen in Fig.4. The $\Gamma(\cdot)$ function assures the time responses of the error between the linear and nonlinear forces to stay bounded. Inside the Δ region where the deviation of lateral tire forces from their linearized values are small, the individual brake torques are equal to zero. Stability analysis is given in Appendix.

2.4 The outer-loop: Steering Controller to Enhance Lateral and Yaw Stability

The outer-loop steering compensation term is calculated by using LQ optimal formulation on a basis of a linearized vehicle model constituted by lateral, yaw and roll dynamics. The state space model of the lateral vehicle model is as follows:

$$\begin{bmatrix} mu & 0 & 0 & -m_s e \\ 0 & I_z & 0 & I_{xz} \\ 0 & 0 & 1 & 0 \\ m_u eu & I_{xz} & 0 & I_{xs} \end{bmatrix} \begin{bmatrix} \dot{\beta} \\ \dot{r} \\ \dot{\phi} \\ \dot{p} \end{bmatrix} = \begin{bmatrix} -(Cy_f + Cy_r) \\ (Cy_r l_r - Cy_f l_f) \\ 0 \\ -(Cy_f + Cy_r)e \end{bmatrix}$$
$$\begin{bmatrix} -mu + \frac{Cy_r l_r - Cy_f l_f}{u} & 0 & 0 \\ \frac{-(Cy_f l_f^2 + Cy_r l_r^2)}{u} & 0 & 0 \\ 0 & 0 & 1 \\ (-mu + \frac{Cy_r l_r - Cy_f l_f}{u})e & -K_\phi + m_s ge & -C_\phi \end{bmatrix} \begin{bmatrix} \beta \\ r \\ \phi \\ p \end{bmatrix}$$
$$+ \begin{bmatrix} Cy_f \\ Cy_f l_f \\ 0 \\ Cy_f e \end{bmatrix} \delta_f \tag{34}$$

where m_s denotes the vehicle sprung mass, e is the distance of the sprung mass center of gravity from the roll center, I_{xz} product moment of inertia on roll and yaw axes, I_{xs} sprung mass moment of inertia on roll axis, ϕ roll angle, p roll rate, β vehicle side slip angle, K_ϕ roll stiffness, C_ϕ roll damping coefficient, g is the inertial acceleration. The state space model given by (34) may be denoted in compact form as follows:

$$E\dot{x} = Fx + G\delta_f \tag{35}$$

where $x = [\ \beta \quad r \quad \phi \quad p\ ]^T$ is the state vector. Arranging (35), the state space model may be represented by

$$\dot{x} = Ax + B\delta_f \tag{36}$$

where $A = E^{-1}F$ and $B = E^{-1}G$ for the non-zero longitudinal velocity values ($u \neq 0$). The error vector is defined as $e = x - x_d$ where $x_d = [\beta_d \quad r_d \quad \phi_d \quad p_d]^T$ is the desired state vector. The desired yaw rate value is given

$$r_d = \frac{u\delta_f}{l_f + l_r + K_u u^2}, \qquad K_u = \frac{m(l_r Cy_r - l_f Cy_f)}{(l_f + l_r) Cy_f Cy_r}$$

The calculated desired yaw rate value has to be limited otherwise during the desired yaw rate's tracking on the low friction road condition, the side slip angle of the vehicle model may deviate in an unfeasible way,(see also Zanten et al. (1995), Zheng et al. (2006)). Desired yaw rate value is limited by measured lateral acceleration value $|r_d| \leq |a_y/u|$. For enhanced lateral maneuvering capability, desired side slip angle, desired roll angle and desired roll rate are chosen as zero i.e. $\beta_d = 0$, $\phi_d = 0$, $p_d = 0$, penalizing the deviation of the vehicle side slip angle, roll angle and roll rate. Considering the active steering control input term denoted by δ_c, the error dynamics are obtained as follows:

$$\dot{e} = \dot{x} - \dot{x}_d = Ae + B\delta_c + Ax_d - \dot{x}_d \tag{37}$$

Considering the third and fourth terms as disturbances, LQ regulator is applied to minimize the cost function given by

$$J = \int_0^\infty \left(e^T Q e + \delta_c^T R \delta_c\right) dt \tag{38}$$

where Q and R are the constant weighting coefficient matrices. The optimal state feedback gain is obtained by solving the Riccati Equation,

$$A^T P + PA - PBR^{-1}B^T P + Q = 0 \tag{39}$$

The state feedback compensation term is given,

$$\delta_c = -R^{-1}B^T P e \tag{40}$$

where $e = [\ \beta \quad (r - r_d) \quad \phi \quad p\ ]$ is the error vector.

3. SIMULATION STUDY

At the simulation stage, the deadzone in the discontinuous functions $\Gamma(e_f)$ and $\Gamma(e_r)$ is chosen to be same constant value, $\Delta = 500N$. A nonlinear double track vehicle model having 14 degrees of freedom is used for simulations. The nonlinear Magic Formula tire model is performed with the numerical values given in Pacejka (2002) whereas the other vehicle model parameters belong to a sedan type vehicle model.

An obstacle avoidance maneuver is simulated. The front wheel angle is varied from its steady zero value to -0.15 rad and then after from -0.15 rad to 0.15 rad in 1.5 seconds. An asphalt dry road pavement is chosen to possibly excite a rollover threat. The initial longitudinal velocity value is 30 m/s (108 km/h). The time-responses of the vehicle side slip angle β and yaw rate r are plotted in Fig. 5 for the scenario when the vehicle motion is controlled by the proposed two-loops regulator and for the uncontrolled case when there is no controller intervening to the vehicle motion dynamics. In the controlled case, the vehicle side slip angle is regulated around its zero value whereas the uncontrolled one deviates largely. Also the controlled yaw dynamics can follow the driver's desired yaw rate. In Fig. 6, the trajectory in the longitudinal direction versus lateral direction is plotted for both of the controlled and uncontrolled simulation scenarios. For comparison purposes, the driver's desired trajectory, which is calculated using the desired yaw rate value r_{des} and

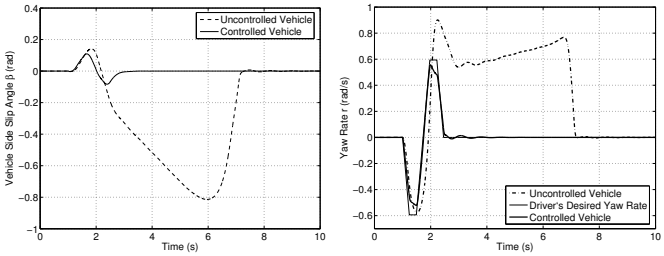

Fig. 5. Left: Vehicle side slip angle. Right: Yaw Rate.

vehicle longitudinal velocity u, is plotted in the same figure. While the uncontrolled vehicle model spins out, the controlled one tracks the driver's desired trajectory closely. In the right side of Fig. 6, the roll angle responses are plotted. The roll angle resumes to zero quickly enhancing lateral stability and cornering capability of the vehicle model. Fig.7 illustrates the change of the vertical tire

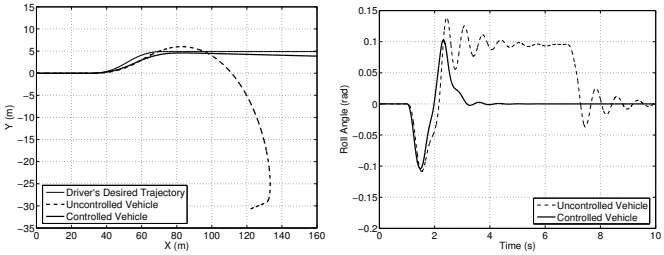

Fig. 6. Left: Trajectories of the vehicle. Right: Change of the roll angles.

forces during the maneuver. In the uncontrolled vehicle, vertical force value reaches to zero illustrating individual wheel handling lost of the rear right tire. Although this doesn't mean a rollover, still it is undesirable for maneuver. In the controlled vehicle, the tire lift off is prevented and the vehicle maneuvers safely without a rollover danger. Fig.8 shows the change of the lateral tire forces during the maneuver with respect to the tire slip angle. The tire force generation is enforced to stay in the linear operating region and hence the handling stability of the vehicle model is improved.

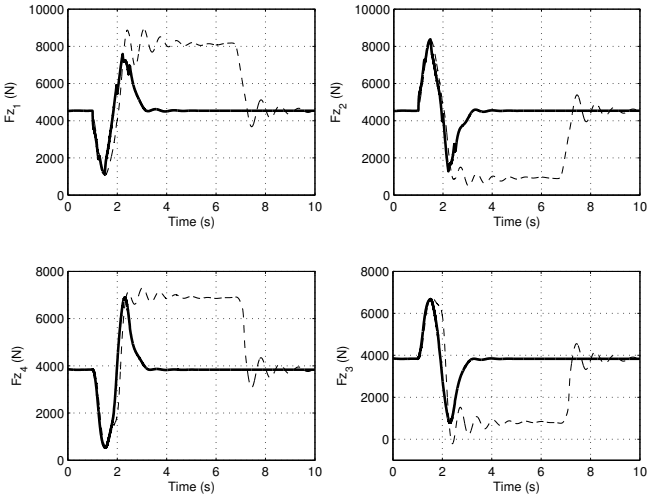

Fig. 7. Change of the tire loads (dashed: uncontrolled vehicle, solid: controlled vehicle).

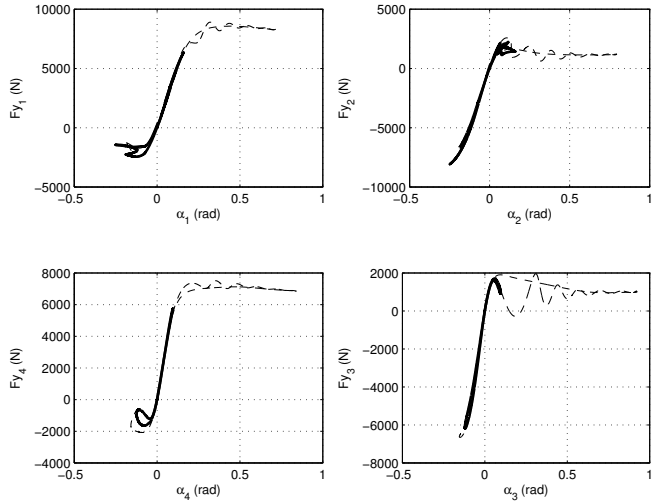

Fig. 8. Change of the lateral tire forces with respect to the tire slip angle (dashed: uncontrolled vehicle, solid: controlled vehicle).

4. CONCLUSIONS

The control algorithm improving vehicle handling and lateral stability is introduced. Handling in the lateral direction is assured by regulating the individually actuated wheel braking actuators preventing the tire force saturation in the lateral direction. The lateral forces generated at the rear and front axle are estimated by using the force estimator in the longitudinal direction whereas they are analytically denoted by the nonlinear functions. In the outer-loop, other input freedom is elaborated to guarantee lateral and yaw stability in an optimal manner. The vehicle motion dynamics in the lateral direction are penalized whereas the yaw rate tracking is assured. Simulation scenarios are performed to validate the effectiveness of the proposed controller during short-term emergency maneuverings.

REFERENCES

T. Acarman, Y. Pan and Ü. Özgüner. A Control authority transition system for collision and accident avoidance. *Journal of Vehicle System Dynamics*, vol. 39(2), pp. 149-187, 2003.

E.Dinçmen, and T.Acarman. Application of Vehicle Dynamics' Active Control to a Realistic Vehicle Model. *Proceedings of the American Control Conference*, pp.200-205, New York City, 2007.

E.Dinçmen, and T.Acarman. Enhancement of Handling and Cornering Capability for Individual Wheel Braking Actuated Vehicle Dynamics. *Proceedings of the Intelligent Vehicle Symposium*, pp.888-893, Istanbul, 2007.

A.T. van Zanten, R. Erhardt, and G. Pfaff. VDC, The Vehicle Dynamics Control System of Bosch. *SAE Technical Paper*, No:950759, 1995.

S. Zheng, H. Tang, Z. Han, Y. Zhang. Controller Design for Vehicle Stability Enhancement. *Control Engineering Practice*, vol. 14(12), pp.1413-1421, 2006.

T. Chung and K. Yi. Design and Evaluation of Side Slip Angle-Based Vehicle Stability Control Scheme on a Virtual Test Track. *IEEE Transactions on Control Systems Technology*, vol. 14(2), pp.224-234, 2006.

Y. Fukada. Slip Angle Estimation for Vehicle Stability Control. *Vehicle System Dynamics*, vol. 32, pp.375-388, 1999.

S. Drakunov, U. Ozguner, P. Dix, and B. Ashrafi. ABS Control Using Optimum Search via Sliding Modes. *IEEE Transc. on Control Systems Technology*, vol. 3(1), pp.79-85, 1995.

H.B. Pacejka. *Tyre and Vehicle Dynamics*. Oxford: Butterworth-Heinemann, 2002.

Appendix. STABILITY ANALYSIS

Lyapunov based stability analysis may be derived in order to prove $e_f \to 0$ and $\dot{e}_f \to 0$ outside the region Δ. Outside of the region Δ, the candidate Lyapunov function $V_f = \frac{1}{2}e_f^2$ is chosen and its derivative with respect to time is given,

$$
\begin{aligned}
\dot{V}_f &= e_f \dot{e}_f \\
&= Cy_f e_f \dot{\alpha}_f - Cy_1 \frac{|\tan\alpha_1|}{(1+\kappa_1)^2} f_1(\lambda_1) k_{11} |\dot{\alpha}_f| |e_f| \\
&- Cy_2 \frac{|\tan\alpha_2|}{(1+\kappa_2)^2} f_2(\lambda_2) k_{21} |\dot{\alpha}_f| |e_f| \\
&- Cy_1 \frac{e_f \dot{\alpha}_1}{\cos^2\alpha_1 (1+\kappa_1)} f_1(\lambda_1) \\
&- Cy_1 \frac{|\tan\alpha_1|}{(1+\kappa_1)^2} f_1(\lambda_1) k_{12} |\dot{\alpha}_1| |e_f| \\
&- Cy_1 \frac{e_f \tan\alpha_1}{1+\kappa_1} \frac{\partial f_1}{\partial \lambda_1} \dot{\lambda}_1 - Cy_1 \frac{|\tan\alpha_1|}{(1+\kappa_1)^2} f_1(\lambda_1) M_1 |e_f| \\
&- Cy_2 \frac{e_f \dot{\alpha}_2}{\cos^2\alpha_2 (1+\kappa_2)} f_1(\lambda_2) \\
&- Cy_2 \frac{|\tan\alpha_2|}{(1+\kappa_2)^2} f_2(\lambda_2) k_{22} |\dot{\alpha}_2| |e_f| \\
&- Cy_2 \frac{e_f \tan\alpha_2}{1+\kappa_2} \frac{\partial f_2}{\partial \lambda_2} \dot{\lambda}_2 - Cy_2 \frac{|\tan\alpha_2|}{(1+\kappa_2)^2} f_2(\lambda_2) M_2 |e_f| \\
&\le \left(Cy_f - Cy_1 \frac{|\tan\alpha_1|}{(1+\kappa_1)^2} f_1(\lambda_1) k_{11} \right. \\
&\quad \left. - Cy_2 \frac{|\tan\alpha_2|}{(1+\kappa_2)^2} f_2(\lambda_2) k_{21} \right) |\dot{\alpha}_f| |e_f| \\
&+ \left(Cy_1 \frac{f_1(\lambda_1)}{(1+\kappa_1)} \right) \left(\frac{1}{\cos^2\alpha_1} - k_{12} \frac{|\tan\alpha_1|}{(1+\kappa_1)} \right) |\dot{\alpha}_1| |e_f| \\
&+ \left(\frac{Cy_1}{1+\kappa_1} \right) \left(\tan\alpha_1 \frac{\partial f_1}{\partial \lambda_1} \dot{\lambda}_1 - \frac{|\tan\alpha_1|}{(1+\kappa_1)} f_1(\lambda_1) M_1 \right) |e_f| \\
&+ \left(Cy_2 \frac{f_1(\lambda_2)}{(1+\kappa_2)} \right) \left(\frac{1}{\cos^2\alpha_2} - k_{22} \frac{|\tan\alpha_2|}{(1+\kappa_2)} \right) |\dot{\alpha}_2| |e_f| \\
&+ \left(\frac{Cy_2}{1+\kappa_2} \right) \left(\tan\alpha_2 \frac{\partial f_2}{\partial \lambda_2} \dot{\lambda}_2 - \frac{|\tan\alpha_2|}{(1+\kappa_2)} f_2(\lambda_2) M_2 \right) |e_f| \\
&\le 0
\end{aligned}
$$

Outside of the region Δ, the time-derivative of the candidate Lyapunov function is always negative since $(1+\kappa_i)$ and $f_i(\lambda_i)$ take always positive values. And also the time derivative of $\frac{\partial f_i}{\partial \lambda_i}\dot{\lambda}_i$ is assumed to be bounded for $i = 1, 2, 3, 4$. Without loose of generality, stability analysis may be derived for the error subjected to the rear axle.